

Polyethylene-supported poly(methyl methacrylate-*co*-butyl acrylate)-based novel gel polymer electrolyte for lithium ion battery

Xueyi Luo¹ · Youhao Liao^{1,2} · Huili Xie¹ · Qiming Huang¹ · Weishan Li^{1,2}

Received: 1 October 2014 / Revised: 14 December 2015 / Accepted: 15 December 2015 / Published online: 6 January 2016
© Springer-Verlag Berlin Heidelberg 2015

Abstract A new copolymer, poly(methyl methacrylate-*co*-butyl acrylate) (P(MMA-*co*-BA)), was synthesized by emulsion polymerization with different mass ratio of methyl methacrylate (MMA) and butyl acrylate (BA). The membranes were prepared by phase inversion and corresponding gel polymer electrolytes (GPEs) were obtained by immersing the membrane into a liquid electrolyte. In this design, the hard monomer MMA provided the copolymer with good electrolyte uptake, while the soft monomer BA provided the GPE with strong adhesion between the anode and cathode of lithium ion battery. The properties of the resulting product were investigated by Fourier transform infrared spectroscopy, nuclear magnetic resonance spectra, scanning electron spectroscopy, linear sweep voltammetry, thermogravimetric analysis, cyclic voltammetry, electrochemical impedance spectroscopy and charge/discharge test. The results show that the obtained GPE based on P(MMA-*co*-BA) with the mass ratios of MMA and BA = 6:1 exhibits good conductivity (as high as $1.2 \times 10^{-3} \text{ S cm}^{-1}$) at room temperature and high electrochemical stability (up to 4.9 V

vs. Li/Li⁺). With the application of the polyethylene (PE)-supported GPE in Li/Li(Li_{0.13}Ni_{0.30}Mn_{0.57})O₂ battery, the battery presents good cyclic stability (maintaining 95.4 % of its initial discharge capacity after 50 cycles) at room temperature.

Keywords Poly(methyl methacrylate-*co*-butyl acrylate) · Polyethylene-supported · Gel polymer electrolyte · Lithium ion battery · Stability

Introduction

More and more attentions have been paid to the application of gel polymer electrolyte (GPE) in lithium ion batteries, dye-sensitized solar cells, fuel cells and super capacitors on account of combining with the advantages of both liquid electrolytes (high ionic conductivity) and solid-state electrolytes (high safety) [1–5]. Currently, most studies of GPE are about lithium ion batteries since its safety problem gives rise to highly concern [6–10]. The safety problem caused by conventional lithium ion batteries using liquid carbonated electrolyte can be solved through absorbing liquid electrolytes as much as possible into the polymer matrixes to reduce its free flow rate inside the battery. Plentiful polymers have been studied so far, including poly(ethylene oxide) (PEO) [11], poly(vinylidene fluoride) (PVDF) [12], polyacrylonitrile (PAN) [13], poly(methylmethacrylate) (PMMA) [14] and polyvinyl chloride (PVC) [15]. However, there exists various drawbacks in these developed polymers and corresponding GPEs. The performances in terms of electrolyte uptake, ionic conductivity and electrochemical stability still need to be improved to meet the requirement of commercial lithium ion batteries. It is reported that

✉ Youhao Liao
liaoyouhao@126.com

✉ Weishan Li
liwsh@scnu.edu.cn

¹ School of Chemistry and Environment, South China Normal University, Guangzhou 510006, China

² Engineering Research Center of MTEES (Ministry of Education), Research Center of BMET (Guangdong Province), Engineering Lab. of OFMHEB (Guangdong Province), Key Lab. of ETESPG (GHEI), and Innovative Platform for ITBMD (Guangzhou Municipality), South China Normal University, Guangzhou 510006, China

above drawbacks can be made up to some extent through copolymerization using hard monomer and soft monomer that have different functions, such as poly(acrylonitrile-vinyl acetate) [P(AN-VAc)] [16] and poly(methylmethacrylate-acrylonitrile) [P(MMA-AN)] [17].

It has been known that the hard monomer, methyl methacrylate (MMA), provides the copolymer with good electrolyte uptake [18], which is mainly responsible for the high ionic conductivity of the GPE. The soft monomer, butyl acrylate (BA), provides the GPE with strong adhesion of the GPE with the anode and cathode of lithium ion battery [19, 20]. In the hope of employing the individuals advantage of MMA and BA, we report the synthesis of poly(methyl methacrylate-co-butyl acrylate) (P(MMA-co-BA)) copolymer for the first time. The properties of the resulting copolymer and corresponding membrane and GPE are investigated. The performance of the developed GPE is evaluated in the Li/Li(Li_{0.13}Ni_{0.30}Mn_{0.57})O₂ coin cell.

Experimental

Preparation

P(MMA-co-BA) was prepared by emulsion polymerization. Commercial monomers, MMA (>99.0 %) and BA (>99.0 %), were distilled in vacuum to remove the aggregation inhibitor. Sodium dodecyl sulphate (SDS) as an emulsifier was dissolved in the deionized water with a concentration of 1.5 wt% to form a homogeneous emulsion solution under N₂ flow at 60 °C in a four-neck glass reactor. The mixture with different mass ratios of MMA and BA was added into the SDS solution under stirring vigorously for 30 min. Sodium persulphate solution as aggregation inhibitor (0.15 wt%, the resulted concentration of the salt in the mixture) was slowly added into the emulsified solution, and then the polymerization was continued for 6 h under vigorous stirring. The resulting emulsion was poured into 3 wt% Al₂(SO₄)₃ solution to yield the precipitate according to the reports [4, 5, 10, 18, 22, 23], which was subsequently filtered, washed with ethanol and then with hot deionized water (40 °C) in order to remove impurities such as residual monomers and emulsifier. The copolymer P(MMA-co-BA) in the form of white powder was finally obtained by drying the purified precipitate in a vacuum at 60 °C for 24 h. Four copolymers were obtained with the mass ratios of MMA to BA 4:1, 5:1, 6:1 and 7:1, respectively. The main synthesis route is shown in Scheme 1.

To improve the mechanical strength of the membrane and corresponding GPE, polyethylene (PE) is used as supporter. The prepared P(MMA-co-BA) copolymer was dissolved at a concentration of 4 wt% in anhydrous dimethylformamide (DMF) at 80 °C for 1 h. After complete dissolution, the

resulting transparent and viscous slurry was cast onto a PE supporter using doctor blade technique, then quickly immersed in deionized water. The porous membrane is formed through the phase inversion due to the exchange of water (non-solvent) and DMF (solvent) with the average pore size of about 0.08 μm. The resulting membrane was washed with deionized water and then immersed in deionized water for 2 h to remove residual DMF. The membrane was finally obtained after drying the membrane in vacuum at 60 °C for 24 h.

In order to obtain GPE, the PE-supported P(MMA-co-BA) membrane was immersed in 1 M LiPF₆ solution employing ethylene carbonate (EC)/dimethyl carbonate (DMC) (EC/DMC = 1/1, v/v, battery grade, Samsung Cheil Industry, Korea) as solvent for 30 min in an argon-filled glove box (Mikrouna). The thickness of the film before the uptake electrolytes is 50 μm in average, while 55 μm after uptake electrolytes.

Characterization

The electrolyte uptake (*A*) of PE-P(MMA-co-BA) membranes with different mass ratio of MMA and BA was characterized by immersing the membranes in 1 M LiPF₆ (EC/DMC = 1/1, V/V) solution for 1 h, and obtained by Eq. (1) according to [4, 5]:

$$A(\%) = \frac{W_2 - W_1}{W_1} \times 100\% \quad (1)$$

where *W*₂ and *W*₁ were the mass of the wet and dry membranes, respectively.

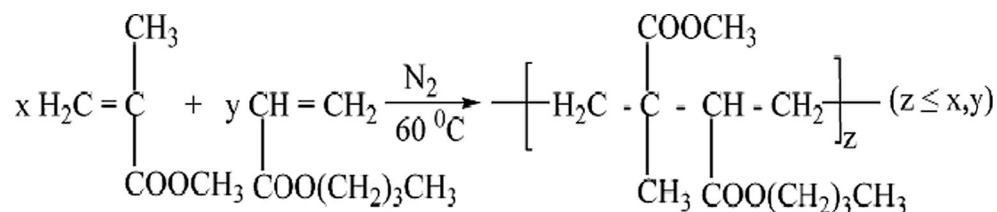
The porosity of membrane was determined by soaking in n-butanol for 2 h until equilibrium was achieved at room temperature. The excess n-butanol adhering to the membrane surface was gently removed with wipes. The porosity (*P*%) was calculated by equation (2) based on [10, 22]:

$$P\% = \frac{W_w - W_d}{\rho_b \times V_m} \times 100\% \quad (2)$$

where *W*_w and *W*_d were the weights of the electrolyte-soaked membrane and dry membrane, respectively, and *ρ*_b was the density of n-butanol and *V*_m was the volume of the dry membrane.

The ionic conductivity of the GPE was measured by ac impedance spectroscopy on electrochemical instrument (PGSTAT-30, Eco Chemie B.V. Company) with a symmetrical cell, SS (stainless steel)/GPE/SS. The GPE was sandwiched between two SS discs (diameter Φ = 16.2 mm). The ionic conductivity was calculated from the bulk electrolyte resistance (*R*) according to [22, 23]:

$$\sigma = \frac{l}{RS} \quad (3)$$

Scheme 1 Synthesis route of copolymer P(MMA-co-BA)

where l was the thickness of the GPE and S was the contact area between GPE and SS disc.

The bulk electrolyte resistance was obtained from the complex impedance diagram. The alternative current signal of the measurement for EIS (electrochemical impedance spectrum) is from 100 kHz to 1 Hz with potential amplitude of 10 mV.

The structure of the copolymer was determined by Fourier transform infrared spectroscopy (FTIR, BRUKER TENSOR 27) in the range of 450–4000 cm^{-1} and nuclear magnetic resonance (NMR) spectra, which were measured in dimethyl sulphoxide (DMSO) solvent using a Bruker AVANCE AV 400 MHz spectrometer. The morphology of the copolymer membrane was characterized by scanning electron microscopy (SEM, JEOL, JSM-6510A, JAPAN) at an acceleration voltage of 15 kV.

The electrochemical stability of the GPE was decided by reduction and oxidation conditions. The reductive stability was determined on Autolab (PGSTAT-30, Eco Chemie B.V. Company) by EIS using the symmetrical cell Li/GPE/Li. In the EIS measurement, amplitude of the alternative current was 5 mV and the frequencies were from 500 kHz to 30 mHz. The oxidative stability of the GPE was conducted on the electrochemical instrument (PGSTAT-30, Eco Chemie B.V. Company) by linear sweep voltammetry (LSV) using the cell Li/GPE/SS with the scanning rate of 1 mV s^{-1} , in which the SS was as working electrode, the lithium as the reference and the counter electrodes. The cyclic voltammetry (CV) measurement was determined on Solartron 1470E (England) using the cell Li/GPE/SS likewise between -0.5 and 5 V at the scanning rate of 1 mV s^{-1} as well.

The thermogravimetric analysis (TGA) was obtained using a NETZSCH TG/DSC analyser (model STA-200PC) to survey thermal stability of the membrane. To determine the cyclic performance of lithium ion battery using the developed GPE, the 2025 coin cell with the structure of Li/GPE/Li(Li_{0.13}Ni_{0.30}Mn_{0.57})O₂ was set up and cycled between 3.5 and 4.9 V at 0.1 C rate using multi-channel battery testers (LAND CT2001A) at room temperature.

To obtain the reproducible results, the data of this work were done with five samples; the reported value was the average one with the error less than 5 %.

Results and discussion

Effect of monomer ratio on electrolyte uptake, porosity and ionic conductivity

The electrolyte uptake of membrane, which is closely related to the monomer ratio of polymer matrix, is crucial for the GPE with high ionic conductivity [21, 22]. The electrolyte uptake of the resulting membranes calculated by Eq. (1) is shown in Fig. 1. The electrolyte uptake of the membrane with the mass ratio of MMA and BA = 6:1 has the largest value, which should be ascribed to the proper ratio of hard monomer (MMA) and soft monomer (BA) during copolymerization reaction. However, increasing or decreasing the ratio of MMA in copolymer, the electrolyte uptake would be reduced. In addition, it can be observed that the electrolyte uptake of membrane with the mass ratio of MMA and BA = 7:1 is second to the best one. Therefore, the further investigation would be conducted on these two ratios of membrane.

For comparison, the porosity of P(MMA-co-BA) membranes with different mass ratios of MMA and BA (6:1 and 7:1) is presented in Fig. 2. The porosity of the membrane with the mass ratios of MMA and BA = 6:1 is 61.1 %, while that of the membrane with the mass ratios of MMA and BA = 7:1 is 59.4 %, which is consistent with the electrolyte uptake, indicating that proper porosity of membrane is beneficial to uptake the electrolyte.

Figure 3 shows the Nyquist plot of the GPEs using PMMA and P(MMA-co-BA) with different mass ratios of MMA and BA as matrix at room temperature. The measurement was carried out on the cell SS/GPE/SS. It can be found that the imaginary part of the impedance is linearly related to its real part. The intersection of the straight line with the real part axis is the bulk electrolyte resistance (R) [5, 14, 21, 22]. At room temperature, the ionic conductivity of GPE based on P(MMA-co-BA) with the mass ratio of MMA and BA = 6:1 is $1.2 \times 10^{-3} \text{ S cm}^{-1}$, while GPEs based on P(MMA-co-BA) with the mass ratio of MMA and BA = 7:1 and PMMA are 1.0×10^{-3} and $0.85 \times 10^{-3} \text{ S cm}^{-1}$, respectively. The result indicates that the improvement in the ionic conductivity for the binary copolymer is achieved through augmenting another monomer with the suitable proportion of the original MMA monomer, while the higher ionic conductivity of

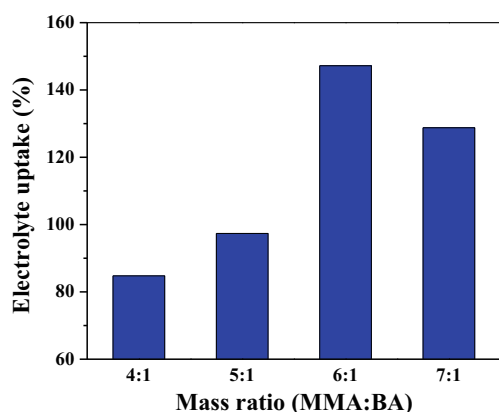


Fig. 1 Dependence of electrolyte uptake of P(MMA-co-BA) membranes on the mass ratios of MMA and BA

P(MMA-co-BA) with the mass ratio of MMA and BA = 6:1 should be ascribed to its interconnected pore structure.

Effect of monomer ratio on electrochemical stability

The compatibility of GPEs with cathode of lithium ion battery was investigated by their electrochemical stability on stainless steel under anodic oxidation. Figure 4 shows the linear sweep voltammograms (LSV) on stainless steel for GPEs based on PMMA and P(MMA-co-BA) with different mass ratios of MMA and BA. From the curve of Fig. 4, it can be seen that the PMMA-based GPE has strong current response at around 4.5 V (vs. Li/Li⁺), while the GPEs based on P(MMA-co-BA) with the mass ratio of MMA and BA = 6:1 and 7:1 are electrochemically stable up to about 4.9 and 4.8 V, respectively. Apparently, the combination between MMA and BA enhances the electrochemical stability. This improvement can be ascribed to the contribution of the branched chain in BA (-(CH)₂-CH₃) to the polymer, which is more important than that of MMA (-CH₃).

To understand whether the developed GPE blocks the reversibility of Li-ion deposition and dissolution or not, the cyclic voltammetry measurement was carried out employing

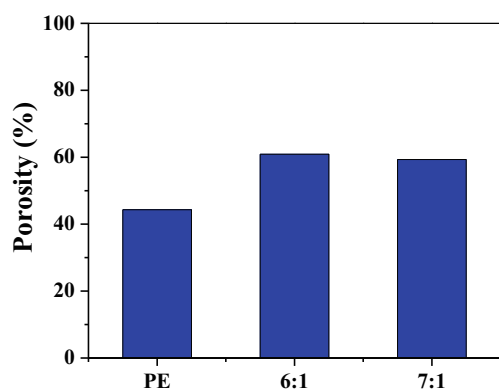


Fig. 2 Porosity of P(MMA-co-BA) membranes with different mass ratios of MMA and BA

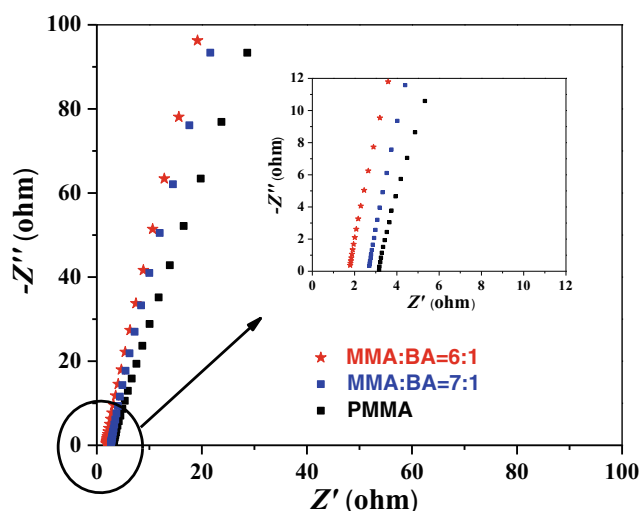


Fig. 3 Nyquist plot of the cell SS/GPE/SS at room temperature. The GPE is based on PMMA and P(MMA-co-BA) with mass ratios of MMA:BA = 6:1 and 7:1

stainless steel as working electrode and lithium foil as reference electrode. Figure 5 presents the cyclic voltammetry of the cell SS/GPE/Li using GPEs based on PMMA and P(MMA-co-BA) with the mass ratio of MMA and BA = 6:1 and 7:1. It is found that there is no obvious difference of the current response on these three GPEs: all of them have an anodic peak at about 0.5 V resulted from the stripping of lithium metal, while the cathodic peak observed at about -0.46 V is caused by the lithium deposition on the stainless steel electrode. In addition, the almost overlapping of CV curves for the first 5 cycles indicate that the highly reversible deposition and dissolution of lithium ion. Thus, the P(MMA-co-BA) based GPE that has reversible redox stability is suitable to apply in current lithium ion battery. In accordance with analysis of the above, the copolymer with optimal mass ratio of MMA and BA = 6:1 shows the best performance on the electrolyte uptake, porosity, ionic conductivity and electrochemical stability; thus, this mass ratio of copolymer was chosen for further investigation.

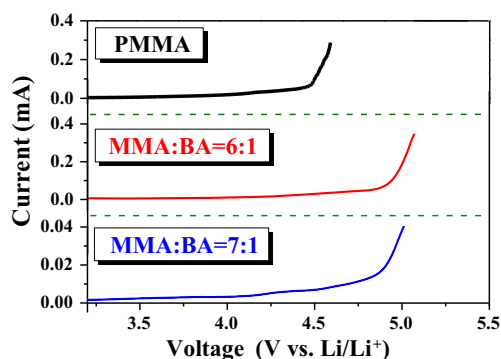
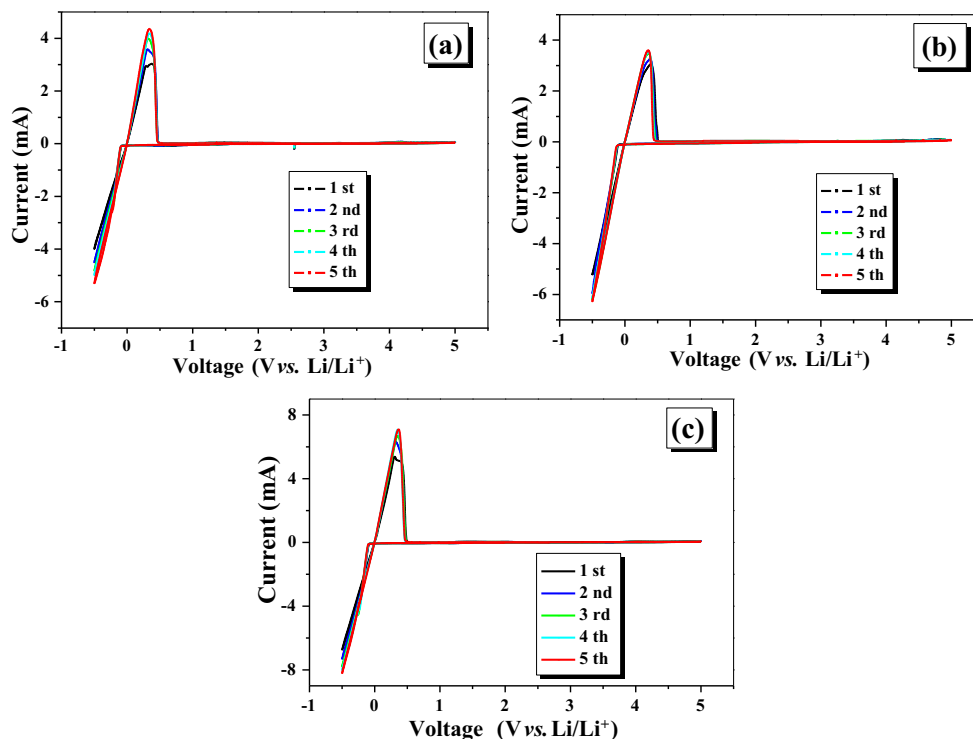


Fig. 4 Linear sweep voltammograms on stainless steel for PMMA and P(MMA-co-BA) with mass ratio of MMA:BA = 6:1 and 7:1-based GPEs, scanning rate 1 mV s⁻¹

Fig. 5 Cyclic voltammogram of Li/GPE/SS cell with the scanning rate of 1 mV s^{-1} . The GPE is based on **a** PMMA and **b** P(MMA-co-BA) with the mass ratio of MMA:BA = 6:1 and **c** P(MMA-co-BA) with the mass ratio of MMA:BA = 7:1



FTIR analysis

Figure 6 presents the FTIR spectra of monomers MMA, BA and their copolymer of P(MMA-co-BA) (mass ratio: MMA:BA = 6:1). It can be seen from Fig. 6 that the characteristic absorption peaks of MMA are at 1643.2 cm^{-1} for the C=C bond and 1737.7 cm^{-1} for the stretching C=O bond [23, 24]. The peaks at 1639.4 and 1733.9 cm^{-1} are corresponded to the C=C bond and C=O bond in BA, respectively. Comparing the FTIR spectrum of the copolymer with those of two monomers, it can be found that the copolymer keeps the absorption peaks at 1739.7 cm^{-1} (C=O), but loses the peaks at 1643.2 and 1639.4 cm^{-1} for C=C bonds in each monomer, suggesting that the copolymer forms through breaking of C=C bonds in each monomers while keeps the main characteristics of the monomers.

NMR analysis

To determine the real ratio of monomers MMA and BA in the copolymer chain, ^1H NMR spectra was carried out. Figure 7c presents the result of ^1H NMR spectra for P(MMA-co-BA) copolymer powder. The peaks seated in the range of 1.0–1.4 and 1.8–2.2 ppm are caused by the response of α -methyl proton (CH_3) and the methylene proton (CH_2) in the copolymer chain, respectively. Strong responded peak at 2.5 ppm is ascribed to the proton in DMSO solvent. Another strong response at around 3.3 ppm should be caused by the proton in H_2O , which may come from DMSO solvent or copolymer. As

can be seen from Fig. 7b, there is a peak at around 3.4–3.6 ppm due to the methoxy proton ($\text{O}-\text{CH}_3$) linked with nearby carbonyl group in the MMA chain [23], while the methylene proton ($\text{O}-\text{CH}_2$) of $-\text{O}(\text{CH}_2)_3\text{CH}_3$ chain in the BA unit results in the peak of around 3.8–4.0 ppm [25]. Based on the integral of each area for characterized proton peaks, it can be calculated that the real ratios of MMA and BA unit in the copolymer is 6:0.9, which is less than the ratios of 6:1 in raw materials, indicating that partial BA monomer did not participate in the emulsion polymerization reaction. It is worth noting in Fig. 7a that there is no other response at around 4.5–5.9 ppm for alkenes proton ($\text{CH}_2=\text{C}$) in the copolymer chains, suggesting that the residual BA monomer is

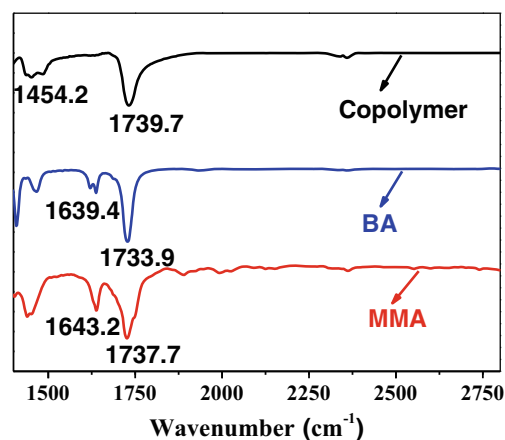
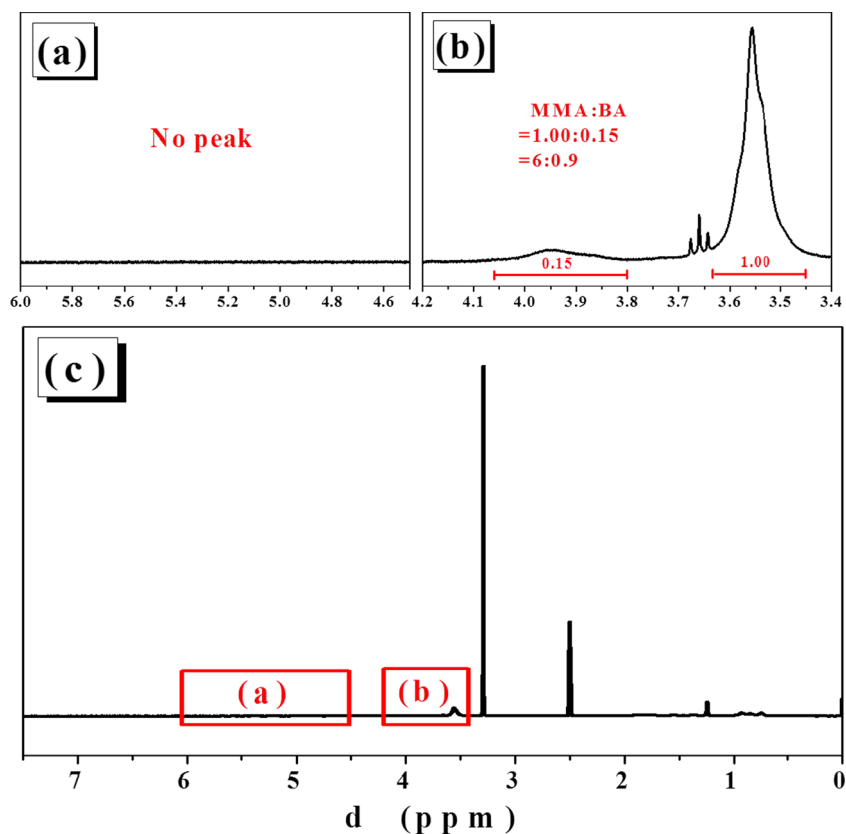


Fig. 6 FTIR spectra of monomers, MMA and BA, and their copolymer P(MMA-co-BA) with the mass ratio of MMA:BA = 6:1

Fig. 7 $^1\text{H-NMR}$ spectra of P(MMA-*co*-BA) copolymer with the mass ratio of MMA:BA = 6:1. **c** is the full scale of the figure, while **a** and **b** is the fractionated section of fig. **a**



removed totally after washing by the deionized water and ethanol. The NMR analysis is also in accordance with that of FTIR result.

SEM image

Figure 8 exhibits the SEM image of the PE-supported P(MMA-*co*-BA) membrane with the mass ratio of MMA and BA = 6:1. The membrane exhibits a dense pore structure in the surface and the interconnected pores under the surface. The average pore size is about $0.08\ \mu\text{m}$, which is suitable for the membrane to absorb proper amount of liquid electrolyte and transport ions, and also helps to reduce the possibility of internal short-circuit in lithium ion battery. The SEM observation of membrane approves that membrane with interconnected pore structure and average pore size is beneficial to its electrolyte uptake, ionic conductivity and electrochemical stability.

Thermal stability

The abuse of battery, taking over-charge and over-discharge for example, will bring about excessive heat, leading to the shrinkage of the membrane and even safety hazard. Thus, the thermal stability of membrane is vital to determine the practical usage of the lithium ion battery. Figure 9 shows the thermal

stability of PMMA membrane and P(MMA-*co*-BA) membranes with the mass ratio of MMA and BA = 6:1, which were analysed by TGA under N_2 atmosphere from 40 to $600\ ^\circ\text{C}$ at a heating rate of $10\ ^\circ\text{C}\ \text{min}^{-1}$. It can be seen that the membrane of P(MMA-*co*-BA) with the mass ratio of MMA and BA = 6:1 is stable up to $300\ ^\circ\text{C}$, compared with the PMMA membrane whose decomposition temperature is $280\ ^\circ\text{C}$, suggesting that introducing BA as secondary monomer into the

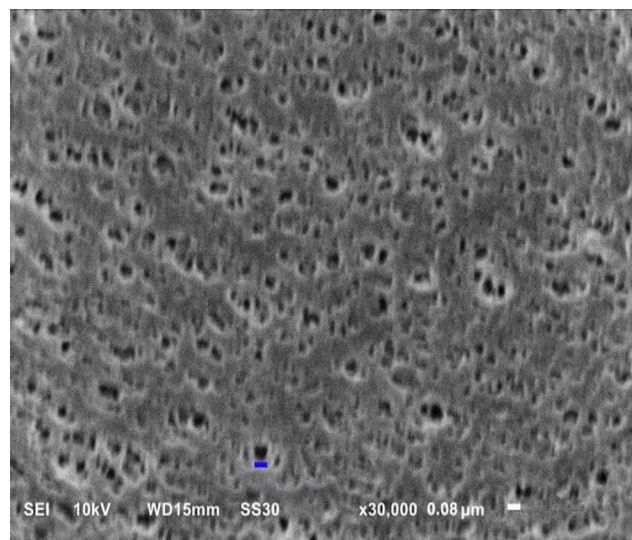


Fig. 8 SEM images of P(MMA-*co*-BA) membrane

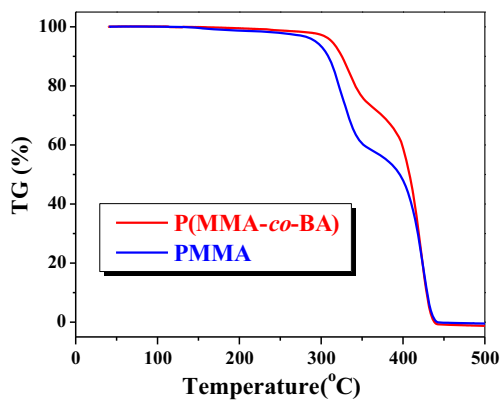


Fig. 9 TG curves of PMMA and P(MMA-co-BA) membranes

membrane could improve the thermal stability of PMMA. In the process of heating, the membrane loses weight by breaking down the C–C and C–H bonds in the copolymer, along with the production of gaseous compounds (CO₂ and H₂O). The promotion of thermal stability for the developed membrane is attributed to the improvement in the bond strength of the copolymer after adding BA monomer.

Compatibility with anode

The compatibility of the GPE with anode of lithium ion battery was evaluated by electrochemical impedance spectra (EIS) [26–28]. Figure 10 shows the EIS for the cells based on the GPEs of PMMA and P(MMA-co-BA) with the mass ratio of MMA and BA = 6:1 at different storage time. It can be seen from Fig. 10 that the impedance spectra is composed of a semicircle at high frequencies, which is related to the contact resistance and charge transfer resistance (the sum of both resistance is considered as the interfacial resistance between electrolyte and electrode), and a short inclined line at low-frequency regions, that belongs to the ion diffusion. As shown in Fig. 10, the interfacial resistance of GPE increases with the storage time, resulted from the continuous growth of a resistive layer on the anode of lithium metal surface. The interfacial resistance of PMMA based GPE enhances from 98 Ω cm² on the first day to 125 Ω cm² after 5 days and 150 Ω cm² after

Fig. 10 Electrochemical impedance spectra of the Li/GPE/Li cell. The GPE is based on a PMMA and b P(MMA-co-BA)

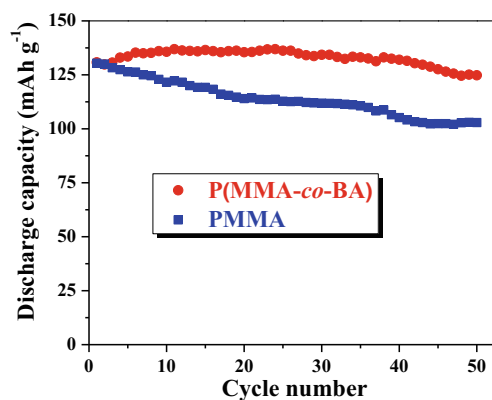
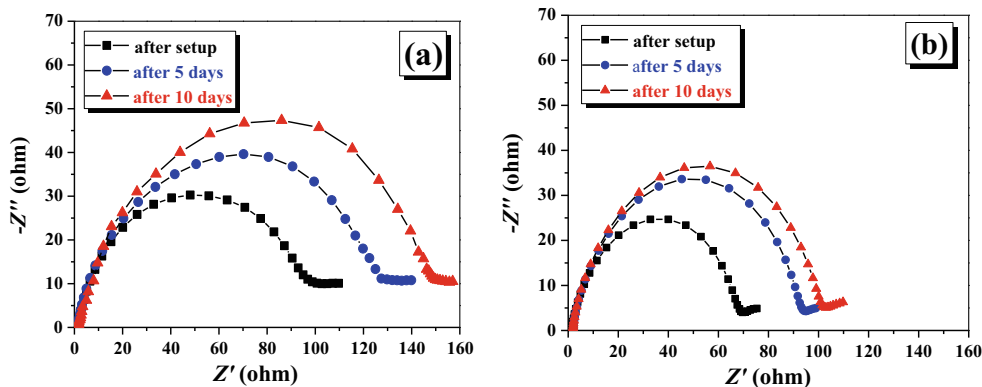


Fig. 11 Cyclic stability of battery Li/GPE/Li(Li_{0.13}Ni_{0.30}Mn_{0.57})O₂ using the GPE based on PMMA and P(MMA-co-BA) polymers

10 days, as shown in Fig. 10a. After introducing soft monomer BA to form the copolymer P(MMA-co-BA), the interfacial resistance of the cell using P(MMA-co-BA) based GPE is 69 Ω cm² on the first day and changes to 94 Ω cm² after 5 days and 105 Ω cm² after 10 days, as shown in Fig. 10b. Although the magnitude of interface resistance both increases for PMMA and P(MMA-co-BA)-based GPE, the growth rate is different. It can be predicted from Fig. 10 that the interfacial resistance of the cell using PMMA-based GPE still has a big growth trend in the later storage time, while that of the cell using P(MMA-co-BA)-based GPE grows slowly since increasing only 9 Ω cm² from the 5th to 10th day. In addition, the interfacial resistance of the cell using P(MMA-co-BA)-based GPE (69 Ω cm²) is obviously less than that of the cell using PMMA-based GPE (98 Ω cm²) on the first day, which indicates that soft monomer BA helps to reduce the growth of resistive layer from the beginning. The activity between developed GPE and lithium metal decreases along with time, thus shows good interfacial stability for the P(MMA-co-BA)-based GPE.

Battery performance

Figure 11 presents the cyclic performance of the Li/Li(Li_{0.13}Ni_{0.30}Mn_{0.57})O₂ coin cells using PMMA and

P(MMA-*co*-BA)-based GPEs. The cell was cycled with a constant current of 0.1 C rate between 3.5 and 4.9 V. After 50 cycles, the cell using P(MMA-*co*-BA) copolymer-based GPE keeps 95.4 % of its initial discharge capacity (declines from 130.8 to 124.8 mAh g⁻¹), which has much higher value than that of the cell using the PMMA oligomer-based GPE, whose capacity retention is 78.9 % (130.4 to 102.9 mAh g⁻¹). For comparison, the current liquid electrolyte-based commercial lithium ion battery with the structure of Li/Li(Li_{0.13}Ni_{0.30}Mn_{0.57})O₂ was fabricated. It can be found that the discharged capacity is decreased from 139.8 mAh g⁻¹ for the initial cycle to 93.6 mAh g⁻¹ after 50 cycles, which has 66.9 % of capacity retention. The result indicates that the lithium ion battery using P(MMA-*co*-BA)-based GPE shows a good cyclic stability, as a consequence of its higher ionic conductivity and better compatibility with electrodes.

Conclusions

Poly(methyl methacrylate-*co*-butyl acrylate) (P(MMA-*co*-BA)) copolymer was successfully synthesized by emulsion polymerization. Transforming the monomer mass ratio of MMA and BA in copolymer influences the performances of corresponding GPEs. Compared with PMMA-based GPE, the P(MMA-*co*-BA)-based GPE with the mass ratio of MMA:BA = 6:1 exhibits preferable characterization in the form of good electrolyte uptake (147.2 %), high porosity (61.1 %), considerable ionic conductivity (1.2×10^{-3} S cm⁻¹) and electrochemical stability (4.9 V), which should be related to its interconnected pore structure and proper pore size. Contributed from the excellent compatibility of GPE with the cathode and anode, the Li/GPE/Li(Li_{0.13}Ni_{0.30}Mn_{0.57})O₂ coin cell using P(MMA-*co*-BA)-based GPE has good cyclic stability, keeping 95.4 % of its initial discharge capacity after 50 cycles. Thus, P(MMA-*co*-BA)-based GPE is a candidate electrolyte for the safer lithium ion battery.

Acknowledgments The authors are highly grateful for the financial support from the National Natural Science Foundation of China (Grant No. 21403076), the joint project of the National Natural Science Foundation of China and the Natural Science Foundation of Guangdong Province (Grant No. U1401248), the Natural Science Foundation of Guangdong Province (Grant No. 2014A030310324) and the scientific research project of the Department of Education of Guangdong Province (Grant No. 2013CXZDA013).

References

1. Agrawal RC, Pandey GP (2008) *J Phys D Appl Phys* 41:223001
2. Quartaronea E, Mustarelli P (2011) *Chem Soc Rev* 40:2525–2540
3. Li ZH, Zhang P, Zhang HP, Wu YP, Zhou XD (2008) *Electrochem Commun* 10:791–794
4. Liao Y, Sun C, Hu S, Li W (2013) *Electrochim Acta* 89:461–468
5. Liao YH, Rao MM, Li WS, Yang LT, Zhu BK, Xu R, Fu CH (2010) *J Membrane Sci* 352:95–99
6. Pu W, He X, Wang L, Tian Z, Jiang C, Wan C (2008) *Ionics* 14:27–31
7. Rajendran S, Shanthi Bama V, Ramesh Prabhu M (2010) *Ionics* 16:27–32
8. Deka M, Kumar A, Deka H, Karak N (2012) *Ionics* 18:181–187
9. Venugopal G, Moore J, Howard J, Pandalwar S (1999) *J Power Sources* 77:34–41
10. Rao MM, Liu JS, Li WS, Liao YH, Liang Y, Zhao LZ (2010) *J Solid State Electrchem* 14:255–261
11. Li H, Ma XT, Shi JL, Yao ZK, Zhu BK, Zhu LP (2011) *Electrochim Acta* 56:2641–2647
12. Zhao YH, Qian YL, Zhu BK, Xu YY (2008) *J Membrane Sci* 310:567–576
13. Amaral F, Dalmolin C, Canobre SC, Bocchi N, Rocha-Filho RC, Biaggio SR (2007) *J Power Sources* 164:379–385
14. Kim HS, Kum KS, Cho WI, Choa BW, Rhee HW (2003) *J Power Sources* 124:221–224
15. Rajendran S, Prabhu MR, Rani MU (2008) *J Power Sources* 180:880–883
16. Rao MM, Liu JS, Li WS, Liang Y, Liao YH, Zhao LZ (2009) *J Power Sources* 189:711–715
17. Zhang P, Zhang HP, Li GC, Li ZH, Wu YP (2008) *Electrochem Commun* 10:1052–1055
18. Liao YH, Zhou DY, Rao MM, Li WS, Cai ZP, Liang Y, Tan CL (2009) *J Power Sources* 189:139–144
19. Luo S, Liu ZH, Liu BL, Liu Q (2011) *Bull Mater Sci* 7:1531–1536
20. Choi YS, Chung IJ (2003) *Macromol Res* 11:425–430
21. Kezuka K, Hatazawa T, Nakajima K (2001) *J Power Sources* 97:98:755–757
22. Liao YH, Rao MM, Li WS, Tan CL, Yi J, Chen L (2009) *Electrochim Acta* 54:6396–6402
23. Sun P, Liao Y, Xie H, Chen T, Rao M, Li W (2014) *J Power Sources* 269:299–307
24. Rzaev ZMO, Güner A, Kibare G, Can HK, Aşıcı A (2002) *Eur Polym J* 38:1245–1254
25. Brar AS, Pradhan DR, Hooda S (2004) *J Mol Struct* 699:39–45
26. Zhou DY, Wang GZ, Li WS, Li GL, Tan CL, Rao MM, Liao YH (2008) *J Power Sources* 184:477–480
27. Momma T, Matsunaga M, Mukoyama D, Osaka T (2012) *J Power Sources* 216:304–307
28. Chai M, Jin YD, Fang SH, Yang L, Hirano S, Tachibana K (2012) *J Power Sources* 216:323–329